CSMA 2026
17ème Colloque National en Calcul des Structures
18-22 Mai 2026, Presqu'île de Giens (Var)

Numerical assessment of a micromorphic approach to approximate cohesive damage gradient models: role of the penalisation factor

Pedro Nava Soto[(1)], Thomas Helfer[(2)], Jean-Michel Scherer[(3)], Olivier Fandeur[(4)], Adrien Jaccon[(5)], Jacques Besson[(6)]

[(1)] *CEA, DES, IRESNE, DEC, SESC, Cadarache, F-13108 Saint-Paul-Lez Durance, France, pedro.NAVASOTO@cea.fr*
[(2)] *CEA, DES, IRESNE, DEC, SESC, Cadarache, F-13108 Saint-Paul-Lez Durance, France, thomas.helfer@cea.fr*
[(3)] *Mines Paris, Université PSL, Centre des Matériaux (MAT), UMR7633 CNRS, Versailles, 78000, Francejean-michel.scherer@minesparis.psl.eu*
[(4)] *Université Paris-Saclay, CEA, Service d'Études Mécaniques et Thermiques, 91191, Gif-sur-Yvette, France, olivier.fandeur@cea.fr*
[(5)] *Université Paris-Saclay, CEA, Service d'Études Mécaniques et Thermiques, 91191, Gif-sur-Yvette, France, adrien.jaccon@cea.fr*
[(6)] *Mines Paris, Université PSL, Centre des Matériaux (MAT), UMR7633 CNRS, Versailles, 78000, Francejacques.besson@minesparis.psl.eu*

Abstract — This paper assesses a micromorphic approach to approximate cohesive damage gradient models. This approach has the advantage of being able to approximate most damage gradient models with a unified finite element implementation, but has the disadvantage of introducing a penalisation coefficient.

Inspired by the current approaches in which a Lagrange multiplier has replaced the penalisation coefficient, and the cell equilibrium algorithm in the context of Hybrid High Order methods, a new numerical strategy is proposed.

Keywords Micromorphic damage model, gradient damage model, cohesive fracture, Hybrid High-Order method.

Introduction

Gradient damage models are widely used in the literature due to their ability to predict crack nucleation, kinking, and bifurcation in brittle materials.

However, a main drawback of the classical AT1 [1] and AT2 [2] models is the rigid definition of the characteristic length, l_c, which is determined by the fracture stress, σ_c, and the fracture energy, G_c. As illustrated in this work, the resulting characteristic length can be too large compared with the structure size, potentially leading to unphysical solutions. To address this issue, Cuvilliez *et al.* proposed a cohesive damage gradient model that allows G_c, σ_c, and l_c to be chosen independently [3].

This paper assesses a micromorphic approach to approximate the cohesive damage gradient model proposed in [3], and applies it to the description of a thermal shock initially proposed by Dharhi *et al.* [4].

The micromorphic approach has the advantage of being flexible: it is able to approximate most of the current gradient damage models by relying on a user-defined behaviour law, thus preserving a unified finite element implementation. However, this approach adds a penalty coefficient [5], which, as will be illustrated in this work, has some limitations.

A new numerical strategy is proposed to address these limitations, inspired by the work of Scherer et al. [6], in which the penalisation coefficient has been replaced by a Lagrange multiplier, and the cell equilibrium algorithm introduced by Siedel et al. in the context of Hybrid High Order methods [7].

1 Micromorphic damage models

1.1 General formulation

As detailed in [5], the micromorphic approach can be described in the standard generalized framework (GSM): to fully characterize the material behaviour, the global free energy Ψ and the dissipation potential Φ must be defined.

1.1.1 Free energy in the medium

The free energy Ψ of the body Ω reads as a function of the strain ε, damage α, micromorphic damage α_χ, and micromorphic damage gradient $\nabla\alpha_\chi$

$$\Psi(\varepsilon,\alpha,\alpha_\chi,\nabla\alpha_\chi) = \Psi_{\varepsilon,\alpha}(\varepsilon,\alpha) + \Psi_\alpha(\alpha) + \Psi_{\alpha,\alpha_\chi}(\alpha_\chi,\alpha) + \psi_{\nabla\alpha}(\nabla\alpha_\chi)$$

Mechanical energy The mechanical energy is defined in the same way as in standard gradient damage models:

$$\Psi_{\varepsilon,\alpha} = (g(\alpha)+\kappa)\Psi_D(\varepsilon) + \Psi_R(\varepsilon) \tag{1}$$

where $g(\alpha)$ is the degradation function, and Ψ_D and Ψ_R correspond to the energy splitting to handle the unilateral condition [8]. Accordingly, the Cauchy stress tensor can be derived from Equation 1 such that

$$\sigma = \partial_\varepsilon\Psi = (g(\alpha)+\kappa)\partial_\varepsilon\Psi_D(\varepsilon) + \partial_\varepsilon\Psi_R(\varepsilon).$$

$\kappa = 1\times10^{-6}$ is introduced to provide a non-zero stiffness that ensures numerical convergence, with negligible influence on the model.

Microdamage energy $\Psi_{\alpha,\alpha_\chi}$ models the coupling between the damage field α and the micromorphic damage field α_χ. In the context of approximating gradient damage models, it can be defined as a penalty term as follows:

$$\Psi_{\alpha,\alpha_\chi} = \frac{H_\chi}{2}(\alpha-\alpha_\chi)^2 \tag{2}$$

The scalar microstress a_χ, which is the conjugate to the micromorphic damage field α_χ, is defined as:

$$a_\chi = \partial_{\alpha_\chi}\Psi = H_\chi(\alpha_\chi-\alpha).$$

Microdamage gradient energy $\Psi_{\nabla\alpha_\chi}$ limits the gradient of the micromorphic damage field. It is defined as follows:

$$\Psi_{\nabla\alpha_\chi} = \frac{A_\chi}{2}\|\nabla\alpha_\chi\|^2.$$

The value of A_χ depends on the characteristic length l_c, controlling the diffusion range, and on the fracture energy G_c, to maintain coherence with the total energy dissipated during fracture.

The vector microstress b_χ, which is the conjugate to the gradient of the micromorphic damage field $\nabla\alpha_\chi$, is defined as:

$$b_\chi = \partial_{\nabla\alpha_\chi}\Psi = A_\chi\nabla\alpha_\chi.$$

Macrodamage energy The free energy density Ψ_α depicts the energy associated with a homogeneous process of damage. Owing to the coupling between the diffused micromorphic

field and the damage field through the coupling term, the damage response must incorporate the characteristic length l_c to ensure that the total dissipation of microscopic and macroscopic fields is consistent with the fracture energy G_c.

The generalized scalar stress Y, which is the conjugate to the damage field α, is naturally defined as the opposite of the derivative of Ψ with respect to α:

$$Y = -\partial_\alpha \Psi = -g'(\alpha)\Psi_D(\varepsilon) - w'(\alpha) + H_\chi(\alpha_\chi - \alpha).$$

1.1.2 Dissipation energy in the medium

The dissipation potential $\Phi(\dot{\alpha})$ accounts for the irreversibility of fracture processes in the medium. In this work, $\Phi(\dot{\alpha})$ is defined as follows:

$$\Phi(\dot{\alpha}) = Y_0\dot{\alpha} + I_{\mathbb{R}_+}(\dot{\alpha})$$

where $I_{\mathbb{R}_+}$ denotes the characteristic function, i.e., $I_{\mathbb{R}_+}(x) = \begin{cases} 0, & x \geq 0, \\ \infty, & x < 0 \end{cases}$.

1.1.3 Micromorphic approximation of variational gradient damage models.

In this section, we recall the micromorphic approximation of the model AT1 proposed by Siedel *et al.* [5], [9] and introduce the approximation used for cohesive models.

	$g(\alpha)$	$\psi_\alpha(\alpha)$	A_χ	H_χ	Y_0	conditions
AT1	$(1-\alpha)^2$	$\frac{3G_c}{8l_c}\alpha$	$\frac{3}{4}G_c l_c$	$\beta\frac{3G_c}{4l_c}$	0	
Lorentz	$\left(\frac{(1-\alpha)^2}{1+(m-2)\alpha+(1+pm)\alpha^2}\right)$	$\frac{3G_c}{8l_c}\alpha$	$\frac{3}{4}G_c l_c$	$\beta\frac{3G_c}{4l_c}$	0	$m \geq p+2 \geq 3$

Table 1: Micromorphic approximation of AT1 and Lorentz model

From Table 1, the coefficient H_χ in the penalty term is defined as a function of the fracture energy G_c, the characteristic length l_c, and the adimensional penalisation factor β. A detailed analysis of the choice of β and its impact on the results is discussed in the following section.

Griffith type energy

One of the main advantages of the phase-field models is their capacity to predict crack nucleation. It was shown in [10] that the uniaxial tension fracture stress σ_c for the AT1 model can be computed by:

$$\sigma_c = \sqrt{\frac{3G_c E}{8l_c}} \tag{3}$$

However, as can be seen in Equation 3, the main limitation of the AT1 model to predict crack nucleation is its inability to choose independently the fracture stress, σ_c, the fracture energy G_c, and the characteristic length l_c.

Cohesive type energy

In this work, the cohesive Lorentz model proposed in [3] is approximated using the micromorphic approach using the functions proposed in Table 1.

The only difference between the AT1 and Lorentz model corresponds to the degradation function $g(\alpha)$. The uniaxial tension fracture stress σ_c corresponds to:

$$\sigma_c = \sqrt{\frac{3G_c E}{8l_c(\frac{m}{2})}} \tag{4}$$

In the Lorentz model, the degradation function depends on the parameters m and p, where, as seen in Equation 4, the value of m can be chosen as a function of σ_c, G_c, and the characteristic length l_c, which can now be chosen independently.

More general cohesive models can be constructed by modifying the free-energy terms of the micromorphic formulation. These models can, for example, approximate the family of cohesive gradient damage models presented in [11].

1.1.4 Numerical resolution

In this work, the alternate minimization algorithm proposed by Siedel *et al.* [9] has been adopted. The numerical simulations were performed using the finite element solver `Manta` [12], coupled to the `MFront` code generator [13] for the implementation of the mechanical and micromorphic behaviours. The implementation was validated through cross-validation with the numerical solver `Z-set` to validate the implementation.

1.2 Comparison of Griffith and cohesive damage gradients models

To illustrate the advantage of gradient damage models with cohesive-type energy, we present the resolution of the Dhahri problem [4] using the micromorphic approach with the standard finite element method for thermal shock problems presented in [14] for $\beta = 300$.

The fracture energy G_c is set to $24.3\,\mathrm{J\,m^{-2}}$, the tensile stress strength σ_c is set to 100 MPa, and the disk radius $R = 6.5 \times 10^{-3}$ m.

In the AT1 model, the characteristic length has to be set to 0.3371 mm in order to respect the desired values for σ_c and G_c.

By contrast, using the Lorentz model, it is possible to define independently the characteristic length, l_c, which is chosen equal to 0.14 mm.

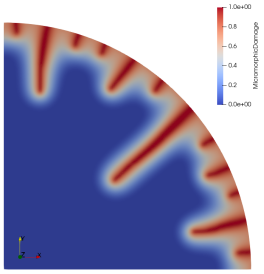

Figure 1: Microdamage at $t = 0.950$s for AT1, $\frac{l_c}{h} = 6.74$

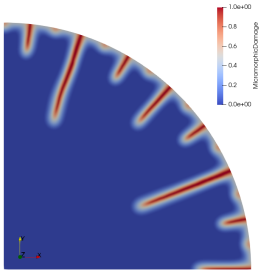

Figure 2: Microdamage at $t = 0.950$s for Lorentz, $\frac{l_c}{h} = 5.6$

Figure 1 and Figure 2 illustrate that the characteristic length l_c used in the AT1 model leads to non-physical crack interactions. The selected value for l_c for the Lorentz model avoids such spurious interactions.

Note that, because each simulation uses a different characteristic length l_c, we employ two different meshes to ensure that $\frac{l_c}{h} > 5$ in both cases. Further details on the choice of the mesh size h and the penalization term $\beta = 300$ are provided in the following section and will be discussed during the oral presentation.

2 Analysis of the penalty factor for approximating cohesive damage gradient models

This section provides an analysis of the impact of the β coefficient.

In the case of the micromorphic approximation of the AT1 and AT2 models, Siedel et al. have shown that a value of $\beta = 300$ allows to obtain accurate predictions of the force-displacement curves in many test-cases in the literature [9], e.g., tension test on a fiber reinforced matrix [15], shear test on a notched plate [16] and shear-driven fracture on a tensile test [17].

In this section, the impact of β on the accuracy of the approximation is studied for cohesive models. We show that this accuracy, for a given value of β, depends on the ratio $\frac{l_c}{h}$ between the characteristic length l_c and the mesh size h.

2.1 Description of one-dimensional tensile test.

The test case consists of a 1 mm bar stretched by a horizontal displacement of amplitude 0.2 mm at the right side, and the left side is clamped. Micromorphic damage is set to zero at both ends of the bar. The material is elastic with $\nu = 0$ and $E = 200\,\mathrm{GPa}$. The brittle fracture properties are $G_c = 1\,\mathrm{J\,m^{-2}}$ and $\sigma_c = 20\,\mathrm{MPa}$. The characteristic length is $l_c = 0.1\,\mathrm{mm}$.

2.2 Analysis of validation results

In this test, the length L of the bar is of intermediate length with respect to σ_c and G_c of the material which implies that the arc-length analytical solution has a snapback phase during crack nucleation from $\sigma_c = 20\,\mathrm{MPa}$ to $5\,\mathrm{MPa}$, followed by a non snapback response for the remainder of the loading until complete failure (see Figures 3 and 4) (see [10] for a more general discussion about the 1D response of gradient damage models and the effect of the bar length).

This induces in the tension test with an increasing load, an unstable crack propagation from $\sigma_c = 20\,\mathrm{MPa}$ to $\sigma_c = 5\,\mathrm{MPa}$ followed by a stable crack propagation until complete failure.

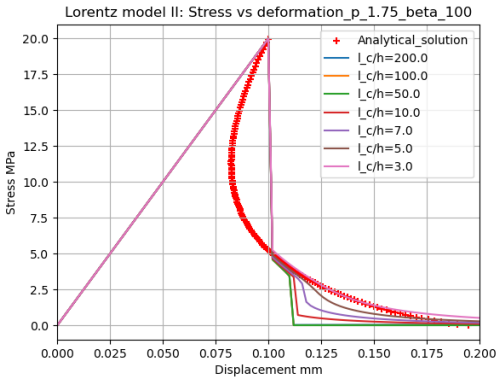

Figure 3: Force vs displacement for $\sigma_c = 20\,\mathrm{MPa}$ and $\beta = 100$

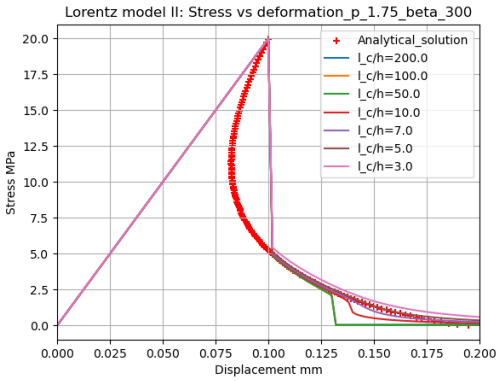

Figure 4: Force vs displacement for $\sigma_c = 20\,\mathrm{MPa}$ and $\beta = 300$

2.3 Results and discussion

In particular, it is shown that the local minima solution of the discretised problem has the following behaviour:

- In the case where the ratio $\frac{l_c}{h}$ is too large for a fixed value of β, the damage field α localises in a one-element band near the peak of the analytical damage profile, which understimates the dissipation.

  Intuitively, for a small enough mesh size, the one-element band localisation of α becomes too small for a fixed value of β to be accurately penalised with the volume microenergy term. This implies the one-element localisation on α is not reproduced by the micromorphic damage field α_χ, thus it is not regularised by the micromorphic gradient energy term.

- For cohesive models, the analytical peak damage value is not necessarily 1 and is fully responsible for the cohesive stress transfer across the crack [2] [3].

For a small enough mesh size, the one-element localisation peak in the damage field α (explained above) fully determines the computed cohesive stress, which leads to an inaccurate representation of the cohesive tension-separation law.

- For a small ratio $\frac{l_c}{h}$, it is possible to fix a β, and the error comes from the expected discretisation error of h to reproduce the regular high gradient analytical solution of the corresponding gradient damage model.

To better understand the dependence of results in β, we recall the micromorphic characteristic length l_χ in [9] [18].

$$l_\chi := \sqrt{\frac{A_\chi}{H_\chi}} = \frac{l_c}{\sqrt{\beta}}$$

And thus, by setting a lower bound in the mesh size $h > 3l_\chi$ which avoids the one-element damage localisation and an upper bound $h < \frac{l_c}{5}$ which ensures an accurate description of the high gradient regularised damage profile, we confirm the choice of $\beta = 300$ in [9] is indeed a good approximation.

3 Toward an Efficient Lagrange-Multiplier Based Implementation of Cohesive Damage Gradient Models

Scherer *et al.* proposed in [6] to enforce weakly the equality of α and α_χ by replacing the penalty coefficient β by a Lagrange multiplier. In particular, Scherer *et al.* highlighted that using a Lagrange multiplier increased the robustness of the simulations [7].

The main disadvantage of this approach, in the context of finite element methods, is that the Lagrange multipliers, defined at the nodes of the mesh, increase the number of unknowns. Moreover, saddle-point problems have issues with many iterative linear solvers required for HPC simulations.

We first recall the main ingredients of the Hybrid high order method and then the basis of the cell equilibrium algorithm introduced by Sieldel *et al.* [9] for the standard micromorphic model.

Finally, we propose to extend the cell equilibrium when Lagrange multipliers are introduced, ensuring that the size of the global problem remains unchanged.

3.1 The Hybrid high order method

We have the following discrete unknowns for the micromorphic field α_χ.

$$\hat{\alpha}_\chi^h := (\alpha_{\chi T}, \alpha_{\chi F})$$

where $\alpha_{\chi T}$ and $\alpha_{\chi F}$ denote the cell and face polynomials, respectively.

The cell unknowns can be eliminated by two approaches:

- static condensation, which consists in applying a Schur complement to eliminate the cell unknowns from the tangent matrix at each step of the Newton method [19]–[21].
- The cell equilibrium is enforced by solving a nonlinear local problem within each cell, thereby eliminating the corresponding unknowns from the global system. [7].

3.2 The equilibrium algorithm

For each estimation of the face unknowns $\alpha_{\chi F}$, the cell unknowns satisfy the following relation:

$$R_T(\alpha_{T\chi}, \alpha_{\chi F}) = 0$$

where R_T is the cell residual associated with the cell equilibrium condition.

The resolution of these problems requires implementing the Newton method at each element prior to the global assembly of the face unknowns. This increases the time and complexity of the cell equilibrium problem, while ensuring that the number of unknowns in the global problem remains unchanged.

3.3 Extension to eliminate Lagrange multiplier

Our approach consists in solving, alongside the cell unknowns α_T, the Lagrange multiplier λ_T, which is determined from the cell equilibrium condition

More precisely, it leads to:

$$R^T(\alpha_\chi^T, \lambda_T, \alpha_\chi^F) = 0$$

A similar approach was proposed in [22] for the elliptic obstacle problem, where piecewise-constant multipliers were used to enforce the obstacle condition on the cell unknowns.

Conclusions and future works

The micromorphic approach was adapted to solve cohesive gradient damage models. The impact of the penalisation factor on the quality of the solution was demonstrated, and we proposed a method to remove this error in the HHO framework [9] by solving the saddle-point problem in [6] at the cell-level.

The validation of the proposed method for different test cases will be shown during the oral presentation.

Acknowledgements This research was conducted in the framework of the MECAN project, which was supported financially by the CEA (Commissariat à l'Énergie Atomique et aux Énergies Alternatives).

References

[1] B. Bourdin, G. A. Francfort, and J.-J. Marigo. Numerical experiments in revisited brittle fracture, Journal of the Mechanics and Physics of Solids, vol. 48, no. 4, pp. 797–826, Apr. 2000.

[2] K. Pham, H. Amor, J.-J. Marigo, and M. Corrado. Gradient Damage Models and Their Use to Approximate Brittle Fracture, International Journal of Damage Mechanics, 2011.

[3] S. Cuvilliez, F. Feyel, E. Lorentz, and S. Michel-Ponnelle. A finite element approach coupling a continuous gradient damage model and a cohesive zone model within the framework of quasi-brittle failure, Computer Methods in Applied Mechanics and Engineering, vol. 237–240, pp. 244–259, Sep. 2012.

[4] M. Dhahri. Etude de la rupture et de l'endommagement par choc thermique des matériaux fragiles et de l'influence des effets dynamiques à partir de l'approche champ de phase, PhD thesis, Université Paris-Nord - Paris XIII ; Université de Tunis El Manar, 2022.

[5] O. Fandeur, T. Helfer, D. Siedel, K. Ammar, and S. Forest. Une approche micromorphe de l'endommagement de matériaux quasi-fragiles : Implémentation numérique et lien avec la méthode par champ de phase, 15ème colloque national en calcul des structures, May 2022.

[6] J.-M. Scherer, V. Phalke, J. Besson, S. Forest, J. Hure, and B. Tanguy. Lagrange multiplier based vs micromorphic gradient-enhanced rate-(in)dependent crystal plasticity modelling and simulation, Computer Methods in Applied Mechanics and Engineering, vol. 372, p. 113426, Dec. 2020.

[7] D. Siedel, T. Helfer, O. Fandeur, J. Besson, S. Forest, and N. Pignet. Schéma de résolution locale pour la méthode Hybrid High Order et application en mécanique non-linéaire, 15ème colloque national en calcul des structures, May 2022.

[8] L. de Lorenzis and C. Maurini. Nucleation under multi-axial loading in variational phase-field models of brittle fracture, International Journal of Fracture, May 2021.

[9] D. Siedel. Une approche numérique robuste pour la description de la rupture fragile et du comportement viscoplastique des crayons de combustible, PhD thesis, Université Paris sciences et lettres, 2023.

[10] J.-J. Marigo and Kim Pham. Construction and analysis of localized responses for gradient damage models in a 1D setting, Vietnam Journal of Mechanics, vol. 31, no. 3–4, Jun. 2010.

[11] J.-Y. Wu. Unified analysis of phase-field models for cohesive fracture. arXiv, Dec. 2024.

[12] O. Jamond *et al.* MANTA: An industrial-strength open-source high performance explicit and implicit multi-physics solver, 16ème colloque national en calcul de structures, May 2024.

[13] T. Helfer, B. Michel, J.-M. Proix, M. Salvo, J. Sercombe, and M. Casella. Introducing the open-source mfront code generator: Application to mechanical behaviours and material knowledge management within the PLEIADES fuel element modelling platform, Computers & Mathematics with Applications, vol. 70, no. 5, pp. 994–1023, Sep. 2015.

[14] P. Nava Soto, O. Fandeur, D. Siedel, T. Helfer, J. Besson, and J.-M. Scherer. Description of thermal shocks using micromorphic damage gradient models, 12th european solid mechanics conference, 2025.

[15] B. Bourdin, G. A. Francfort, and J.-J. Marigo. The Variational Approach to Fracture, Journal of Elasticity, vol. 91, no. 1, pp. 5–148, Apr. 2008.

[16] C. Miehe, F. Welschinger, and M. Hofacker. Thermodynamically consistent phase-field models of fracture: Variational principles and multi-field FE implementations, International Journal for Numerical Methods in Engineering, vol. 83, no. 10, pp. 1273–1311, 2010.

[17] R. Alessi, F. Freddi, and L. Mingazzi. Phase-field numerical strategies for deviatoric driven fractures, Computer Methods in Applied Mechanics and Engineering, vol. 359, p. 112651, Feb. 2020.

[18] S. Forest. Micromorphic Approach for Gradient Elasticity, Viscoplasticity, and Damage, Journal of Engineering Mechanics, vol. 135, no. 3, pp. 117–131, Mar. 2009.

[19] M. Abbas, A. Ern, and N. Pignet. Hybrid High-Order methods for finite deformations of hyperelastic materials, Comput. Mech., vol. 62, no. 4, pp. 909–928, Oct. 2018.

[20] M. Abbas, A. Ern, and N. Pignet. A Hybrid High-Order method for incremental associative plasticity with small deformations, Computer Methods in Applied Mechanics and Engineering, vol. 346, pp. 891–912, Apr. 2019.

[21] M. Abbas, A. Ern, and N. Pignet. A Hybrid High-Order method for finite elastoplastic deformations within a logarithmic strain framework, International Journal for Numerical Methods in Engineering, vol. 120, no. 3, pp. 303–327, 2019.

[22] M. Cicuttin, A. Ern, and T. Gudi. Hybrid high-order methods for the elliptic obstacle problem, Journal of Scientific Computing, vol. 83, no. 8, Mar. 2020.